AIP Journal of Renewable and Sustainable Energy

ZnO based quantum dot sensitized solar cell using CdS quantum dots

Neetu Singh, R. M. Mehra, Avinashi Kapoor, and T. Soga

Citation: J. Renewable Sustainable Energy **4**, 013110 (2012); doi: 10.1063/1.3683531
View online: http://dx.doi.org/10.1063/1.3683531
View Table of Contents: http://jrse.aip.org/resource/1/JRSEBH/v4/i1
Published by the American Institute of Physics.

ZnO based quantum dot sensitized solar cell using CdS quantum dots

Neetu Singh,[1] R. M. Mehra,[2] Avinashi Kapoor,[1] and T. Soga[3]
[1]*Department of Electronic Science, University of Delhi South Campus, New Delhi 110021, India*
[2]*School of Engineering and Technology, Sharda University, Greater Noida 201306, Uttar Pradesh, India*
[3]*Graduate School of Engineering, Nagoya Institute of Technology, Gokiso-cho, Showa-ku, Nagoya 466-8555, Japan*

(Received 29 September 2011; accepted 14 January 2012; published online 8 February 2012)

This paper reports the fabrication of Zinc Oxide (ZnO) based quantum dot sensitized solar cell using Cadmium Sulphide (CdS) quantum dots (QDs) capped by poly vinyl alcohol (PVA). Chemical route was used to synthesize ZnO nanoparticles (NPs) as well as CdS QDs. The crystallite size of ZnO NPs was obtained to be 28 nm at 7 pH. The size of QDs decreased from 5.6 to 2.6 nm with increase in the PVA concentration from 2 to 10 wt. %. There is a blue shift in the band gap of QDs with increase in the concentration of PVA. Current-Voltage characteristic of the cell was obtained and various solar cell parameters were estimated. The efficiency of quantum dot sensitized solar cells was found to be 1.3% at AM 1.5. © *2012 American Institute of Physics*. [doi:10.1063/1.3683531]

I. INTRODUCTION

Quantum dot sensitized solar cells (QDSSCs) have attracted extensive interest as a means of fabricating highly efficient, stable and low cost photovoltaic device because of the tuneable bandgap of the quantum dots.[1] From the last few decades, most of the research in the field of solar energy are focused on dye sensitized solar cells (DSSCs) in which the problem of wastage of photon energy above the difference between lowest unoccupied molecular orbital (LUMO) and highest occupied molecular orbital (HOMO) energies is dominant, because one photon gives rise to one exciton only and rest of the energy contained in the photon is wasted as heat.[2–5] Quantum dots (QDs) have specific advantages over dyes to be used as sensitizers in DSSCs. It is observed that if dye in DSSC is replaced by QDs, then the energy contained in a photon can be fully utilized because in QDs single photon gives rise to multiple excitons.[6,7] This effect is known as multiple exciton generation (MEG) effect. The production of multiple excitons by a single photon in quantum-confined systems may improve the efficiency of solar cells. Researchers have already accomplished the production of 2 or more excitons per photon with energy greater than the bandgap in a PbSe QD based system.[8]

The sensitization in QDSSC is based on the band gap alteration due to the quantum confinement effect (QCE). The absorption edge of QDs can be tailored by exploiting quantum-confined regime of different sized QDs. The bandgap of the QDs can be tuned by controlling their size, and therefore, the absorption spectra of the QDs can be tuned to match the spectral distribution of the sun light.[1,8] QDs can be embedded on front TiO_2/ZnO electrode to achieve enhanced light harvesting in the visible spectrum. However, in spite of the fact that different sized (different bandgap) QDs are available, the energy conversion efficiency of QDSSCs is still low. The less conversion efficiency of the QDSSCs may be due to the difficulty of embedding the QDs into the mesoporous TiO_2/ZnO structure. Another problem is the selection of efficient electrolyte in which the QDSSC can function without degradation. But if suitable linking molecule which could link QDs to TiO_2/ZnO surface and electrolyte be used, then QDs can be used to improve the efficiency of DSSCs.

Much research has been done on the fabrication of QDSSCs in which QDs are embedded in mesoporous TiO_2/ZnO structure by CBD method. Sudhagar *et al*. have reported nanospherical TiO_2 mesoporous layer combined with CdS QDs as a QDSSC application and the resulting efficiency was 1.2%.[9] Chang *et el*. have reported a energy conversion efficiency of 1.84% using I^-/I_3^- electrolyte in CdS based QDSSC.[10] Zhang *et al* have reported a maximum power conversion efficiency of 0.34% for 10 CBD cycles of CdS/ZnO nanowire system.[11] Tak *et al*. have reported the CdS/ZnO nanowire structure as an enhanced photocatalytic activity, because the CdS/ZnO system can efficiently separate photogenerated electron-hole pair and reduce their recombination.[12] Chen *et al* have reported an efficiency of 1.4% in CdS and CdSe co-sensitized QDSSC based on ZnO nanowire.[14]

In the present work, ZnO nanoparticles (NPs) and CdS QDs were synthesised via chemical route. Synthesized ZnO NPs were successfully used as front ZnO electrode in QDSSC. Effect of poly vinyl alcohol (PVA) concentration on structural and optical properties of QDs was investigated. Various parameters of CdS sensitized solar cell were calculated.

II. EXPERIMENTAL

All the reagents used were of analytical grade and no further purification was done before use.

A. Synthesis of ZnO NPs

Zinc acetate dihydrate [99.5% $Zn(CH_3COO)_2.2H_2O$, Alfa Aesar] was used as Zinc precursor. The sol was prepared by dissolving 0.2M of zinc acetate dihydrate in methanol at room temperature. A clear and transparent sol with no precipitate and turbidity was obtained by ultrasonic stirring of the solution for 2 h. NaOH (0.1N, Alfa Aesar) was then added to the sol to adjust the pH level of the sol to 7.[15] The so modified sol was again stirred ultrasonically for 1 h at room temperature.[16] The pH value of the sol was adjusted to add the desired value of OH^- ions in the sol. The clear sol was filtered and kept for complete gelation and hydrolysis process till ZnO precipitate slowly crystallized and settled down at the bottom of the flask. The white precipitate was filtered and washed with excess methanol to remove the starting materials. Precipitate was dried at 80 °C for 15 min on hot plate and ground for 30 min in mortar pestle. The nanopowder so obtained was annealed at 450 °C for 4 h in air by microprocessor controlled annealing furnace with the annealing rate 4 °C/min.

B. Synthesis of CdS QDs

Cadmium chloride (99.9% $CdCl_2$, Alfa Aesar) was used as cadmium source. Sodium Sulphide (99% Na_2S, Alfa Aesar) was used as reducing agent. Poly vinyl alcohol (86–89% PVA, Alfa Aesar) was used as capping agent. Nanoparticles formed during the process need to be surface passivated, as colloids formed in liquid have a tendency to coagulate. Therefore, a capping agent is used to achieve stability and avoid coalescence. PVA is used as capping agent because of its excellent emulsifying property because of which it controls and stabilizes the particle formation by increasing the kinetic stability of the reactants.[17] 20 ml of $CdCl_2$ (0.1M), 20 ml of Na_2S (0.1M), and 20 ml of 10 wt. % PVA solutions were made in deionized (DI) water. $CdCl_2$ was added to PVA solution and stirred continuously. Na_2S was then added to the above solution and again stirred ultrasonically for 1 h. The experiment was repeated for 5 wt. % and 2 wt. % of PVA. The chemical reaction taking place is

$$CdCl_2 + Na_2S \rightarrow CdS + 2NaCl. \quad (1)$$

The solution was kept undisturbed till the precipitate was collected at the bottom. Precipitate was then filtered and dried on hot plate at 60 °C for 15 min. The dried precipitate after grinding was annealed at 150 °C for 30 min. The colour of CdS QDs changed from light yellow to orange with decreasing PVA concentration.

C. Preparation of ZnO electrodes

ZnO nanopowder (1.2 g) was ground by a mortar and pestle with 4 ml DI water and polyethylene glycol ($PEG_{20,000}$, 0.5 g, Alfa Aesar). PEG was used to break up the aggregated particles into a dispersed paste. Thus, prepared uniform slurry was coated on indium tin oxide (ITO) glass by doctor blade technique using an adhesive scotch tape to control the thickness of the ZnO film[18,19] and to provide non-coated areas for electrical contact as spacers. After natural drying at room temperature, the film was sintered in air at 450 °C for 30 min.

D. Preparation of gel electrolyte

The gel electrolyte was prepared by using 10% polyethylene oxide (PEO 99%, Alfa Aesar) solution in acetonitrile and carbon nanotube (CNT, 90+ %, Alfa Aesar) with LiI 0.1M (9.95%, Alfa Aesar), and I_2 0.015M (99.8 %, Alfa Aesar). The whole mixture was placed for sonication to disperse the CNTs into the matrix of polymer. The mixture was stirred for 10 h by a magnetic stirrer for complete mixing between CNTs and polymer molecules.

E. Fabrication of QDSSC

To fabricate QDSSC, prepared ZnO film electrode was first immersed in mercapto propionic acid, which acts as linker molecule between ZnO film electrode and QDs.[20] The modified ZnO electrode was immersed in CdS QD colloidal solution consisting of all the three synthesized QDs. The colloidal solution was formed in toluene by ultrasonication for 2 h. The electrode was immersed in QD solution for 24 h at room temperature. The QD adsorbed electrode was then rinsed with toluene and dried at room temperature. To minimize adsorption of impurities from moisture in the ambient air, the electrode was dipped in the QD solution, while it was still warm (~80 °C). The colour of ZnO electrode changes to yellow after adsorption of CdS QDs. I^-/I_3^- electrolyte was spread on the QD coated ZnO electrode.[21,22] A sandwich type QDSSC was fabricated with the CdS QDs sensitized ZnO electrode, a thin platinum sheet as counter electrode, a spacer, and an electrolyte. The schematic diagram of QDSSC is shown in Figure 1.

In QDSSCs, semiconductors such as CdS, CdSe, PbS, and InP which absorb light in visible region work as sensitizers because they are able to transfer electrons to wide bandgap semiconductors such as ZnO, TiO_2, SnO_2, etc.[8–14] The energy level diagram of QDSSC is shown in Figure 2. The working principle of QDSSC is based on excitation of QDs by photons of light and fast electron injection into the conduction band of ZnO.[23] The injected electron in the conduction band of ZnO percolates through the porous ZnO structure and is fed to the ITO layer which acts as the charge collecting electrode in the cell. The porous ZnO electrode is typically

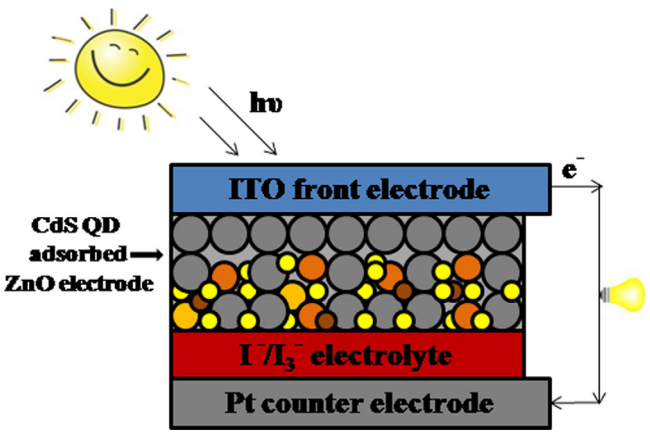

FIG. 1. Schematic diagram of QDSSC.

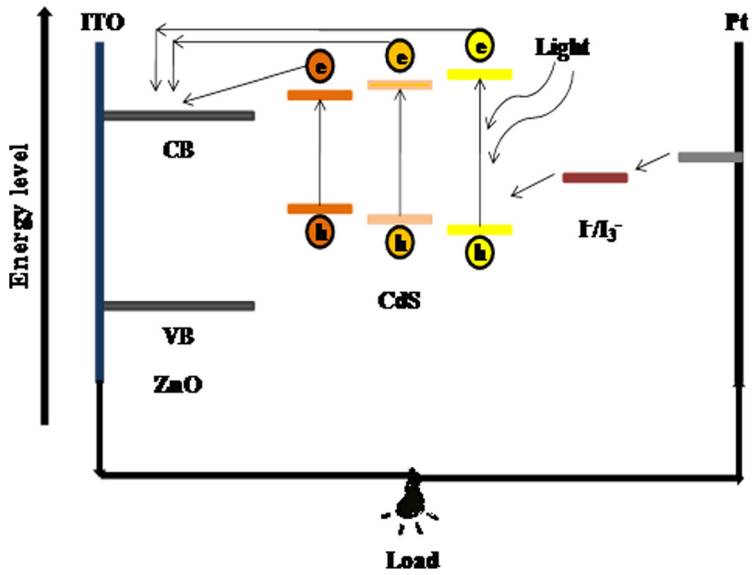

FIG. 2. Energy level diagram of QDSSC.

10 μm thick. Through ITO, the electron moves to the external circuit. At the Pt counter electrode, triiodide (I^-/I_3^-) is reduced to iodide (I^-) by taking the electrons from Pt electrode. I^- is transported through the electrolyte towards the ITO photoelectrode, where it reduces the oxidized QD. The QD is then ready for next excitation/oxidation/reduction cycle. We can see that the working mechanism of QDSSC is similar to that of DSSC, the only difference being that in QDSSC dye is replaced by QDs of varying size by which more light can be harvested and hence the overall efficiency of the cell can be improved.

F. Characterization and I-V measurement

X-ray diffraction (XRD) measurements of the ZnO NPs and CdS QDs were carried out using Bruker AXS – D8 discover diffractometer having CuK_α incident beam ($\lambda = 1.54$ Å). Structural properties of ZnO NPs and CdS QDs were observed by using TECNAI G^2 T30, u-TWIN TEM. The absorbance of ZnO NPs, CdS QDs, and CdS QD embedded ZnO electrode in the visible region was measured using Shimadzu solidspec-3700 UV-VIS-NIR spectrophotometer. I–V characteristic of the cell was measured using computerised digital 2400 Keithley source meter and a M-91190 Newport class-A solar simulator. The measurement was made at AM 1.5. The active electrode area was typically 1 cm^2.

III. RESULT AND DISSCUSSION

A. Analysis of ZnO NPs

The XRD pattern of the synthesized ZnO NPs is shown in Figure 3. The intensity of the diffraction peaks is very high showing that NPs are highly crystalline in nature. The strong diffraction peaks appear at 31.8°, 34.3°, and 36.5°, which correspond to (100), (002) and (101) planes respectively indicating the hexagonal wurtzite structure of ZnO. The preferred orientation corresponding to the plane (101) is shown as the most dominating peak.[24,25] Besides these dominant peaks, other characteristic peaks of ZnO are also there, showing that NPs have grown in all these orientations but maximum growth has occurred in (101) plane. All the diffraction peaks coincide with JCPDS card no. 36-1451 for ZnO powder. No characteristic peak of impurity was observed stating the fact that the synthesized NPs are contamination free and will help not degrading the performance of QDSSC due to impurity elements. Crystallite size (D) was calculated by Debye-Scherrer's formula[26]

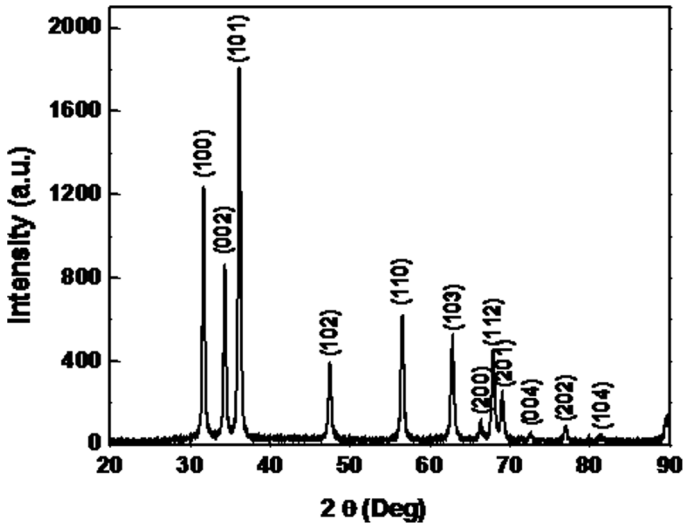

FIG. 3. XRD pattern of ZnO NPs.

$$D = \frac{K\lambda}{\beta \cos\theta}, \tag{2}$$

where, K is the particle shape factor which depends on the shape of the particles and its value is 0.94 for spherical particles, β is the full width at half maximum (FWHM) of the selected diffraction peak corresponding to (101) plane, and θ is the Bragg's angle obtained from 2θ value corresponding to the same plane. Crystallite size of ZnO NPs is calculated to be 28 nm.

Transmission electron microscope (TEM) image of the ZnO NPs is shown in Figure 4(a). A drop of ZnO solution in methanol was drop-cast on a carbon coated copper grid and dried for 1 h before testing through TEM. TEM image mainly consists of hexagonal shaped NPs having an average particle size of approximately 28 nm confirming the results obtained by XRD. SEM image of ZnO electrode is shown in Figure 4(b). The image clearly exhibits the porous nature of the ZnO layer. This porous structure of ZnO helps in the sensitization of QDs in QDSSC because when QDs are embedded on ZnO electrode, QDs actually go and sit in these pores where they get adsorbed (Fig. 1). That is why the cell is known as quantum dot sensitized solar cell because when light falls on such structure, ZnO electrode on the top does not absorb light in the visible region (large bandgap ~3.37 eV) but passes it into the next QD layer where it gets absorbed and sensitizes the dots.

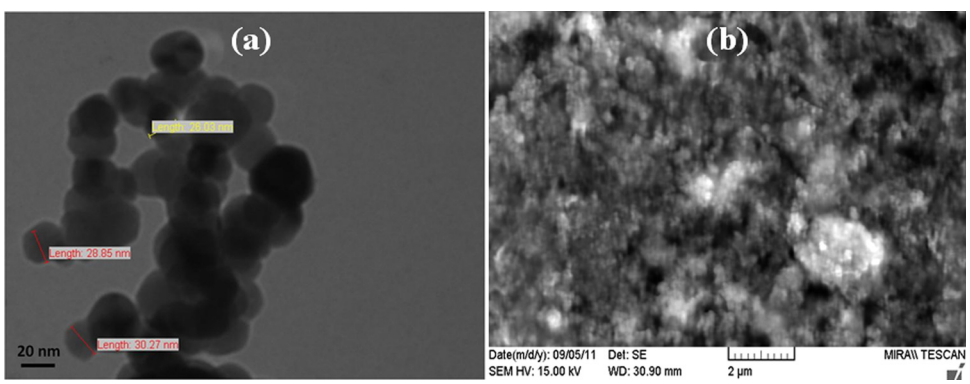

FIG. 4. (a) TEM and (b) SEM images of ZnO NPs.

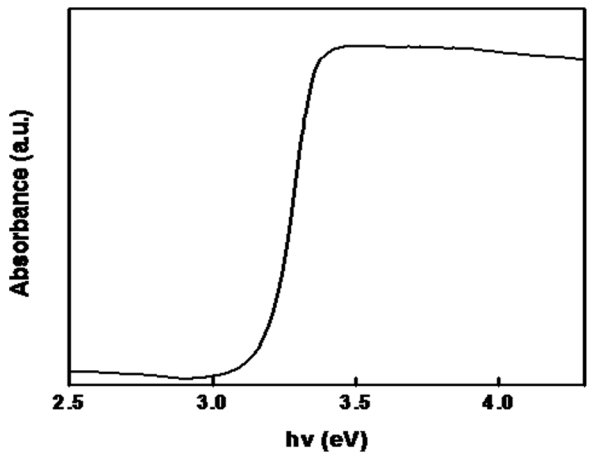

FIG. 5. Optical absorption spectra of ZnO as a function of energy.

The optical absorption spectra of ZnO NPs as a function of energy in the visible region are shown in Figure 5. Graph shows that ZnO does not absorb light in the visible region, which means that prepared ZnO samples are transparent to visible light. We can see that proper light absorbance takes place above bandgap energy of approximately 3.4 eV. Below this energy, absorption level decreases stating that below 3.4 eV photons does not possess enough energy to excite the electrons from valence band to conduction band. The overall analysis of the absorbance spectrum concludes that the synthesized ZnO NPs can be successfully used as a photoelectrode in QDSSC.

B. Analysis of CdS QDs

XRD pattern of CdS QDs with different concentration of PVA is shown in Figure 6. XRD pattern reveals that the dot size is dependent on concentration of PVA. As the PVA concentration increases, the FWHM also increases thereby decreasing the dot size. The dominant peak position is observed at 26.6° for (002) plane, which belongs to hexagonal structure of CdS QDs.[27,28] Two more additional peaks are observed at 43.7° and 51.7° corresponding to (110) and (112) planes, respectively. Dot size is calculated using Debye-Scherrer's formula.[29] The size of the CdS QDs decreases from 5.6 to 2.6 nm with increase in the PVA concentration from 2 to 10 wt. %. The synthesis of QDs, using polymeric stabilizers such as PVA is very easy and requires ambient laboratory conditions.[30–35] The three-dimensional network of the polymer chains efficiently restricts the particle formation to nanoscale. For this purpose, a water-soluble monomer or a polymer compound is generally employed, along with the reagents required for

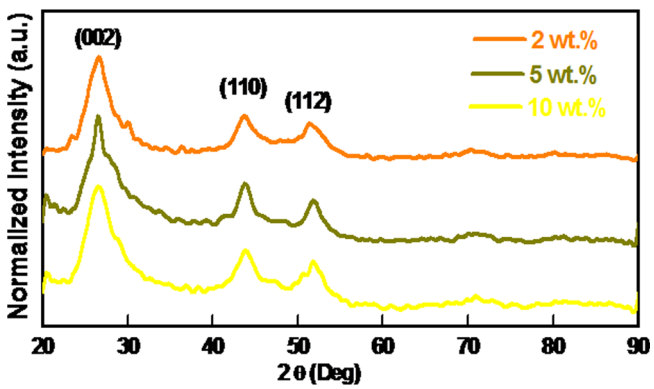

FIG. 6. XRD pattern of CdS QDs with different PVA concentration.

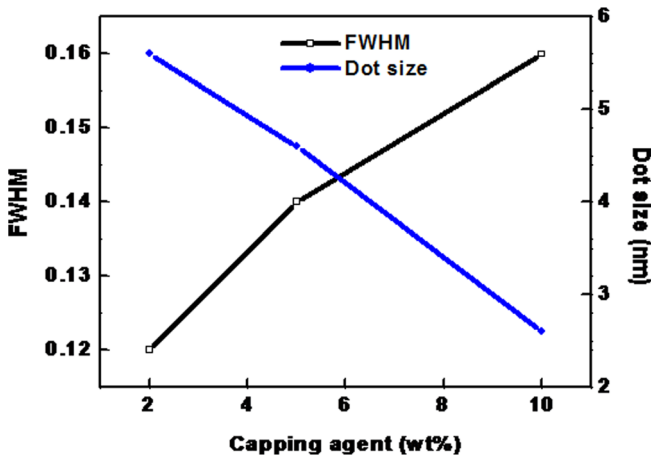

FIG. 7. Effect of PVA concentration on FWHM and size of CdS QDs.

the synthesis of the QDs.[30–36] Recently researchers have used PVA, to stabilize CdSe QDs.[17] The higher concentration of PVA increases the rate of reaction and thus uniform and smaller sized dots are formed.[34]

The variation in FWHM and dot size with capping agent concentration is shown in Figure 7. FWHM increases with increase in the concentration of PVA thereby decreasing the size of the dot. TEM analysis was further carried out to investigate more about CdS phase. TEM images of CdS QDs with different PVA concentration are shown in Figure 8. From the TEM images, it can be seen that the particle size varies from 5.6 to 2.6 nm with increase in the PVA concentration from 2 to 10 wt. %. Therefore, TEM results confirm that the size of the QDs is similar to the dot size obtained by the XRD measurements. The selected area electron diffraction pattern (SAED) of the QDs is also shown in the inset. From the SAED pattern, it is clear that the QDs are crystalline in nature.

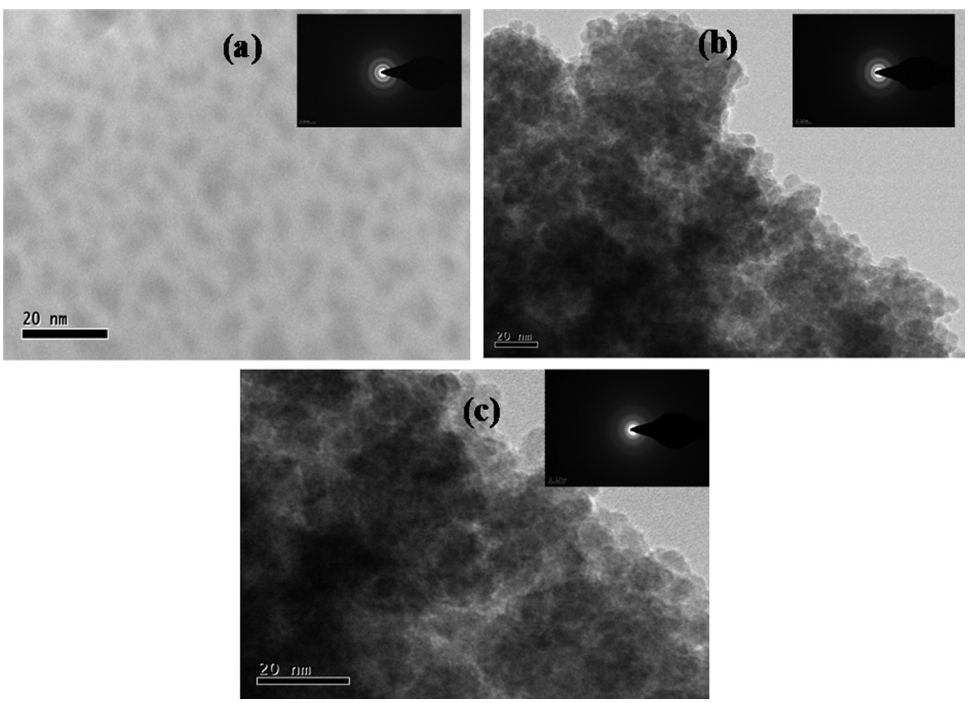

FIG. 8. TEM images CdS QDs with different PVA concentration (a) 2 wt. % (b) 5 wt. %, and (c) 10 wt. %. Inset: SAED of the CdS QDs.

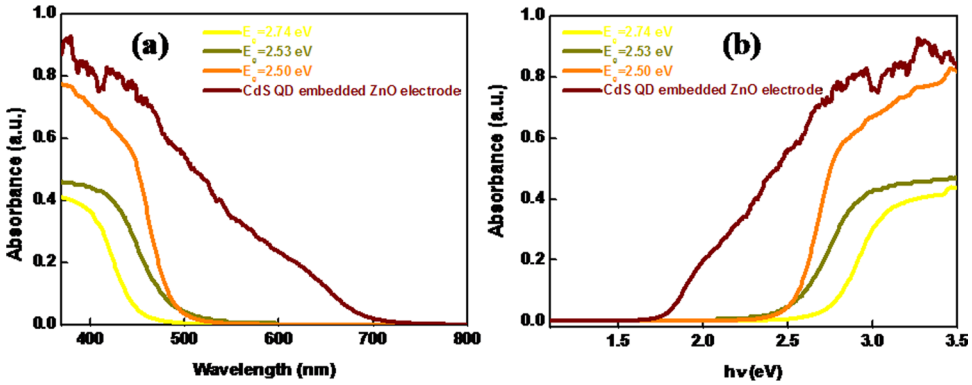

FIG. 9. Optical absorption spectra CdS QDs for various PVA concentration and CdS embedded ZnO electrode.

The optical absorption spectra of the CdS QDs of varying size and CdS QDs embedded on ZnO electrode are shown in Figure 9. Absorbance spectra reveal that there is a blue shift in the absorbance as the dot size decreases due to quantum confinement effect.[37,38] Bandgap of the QDs increases from 2.5 to 2.74 eV with decrease in dot size from 5.6 to 2.6 nm. It is seen from the figure that the absorbance of the CdS QD embedded ZnO electrode covers a wide range of visible spectrum (400–600 nm). Thus using CdS QDs as sensitizers onto ZnO NPs resulted enhanced light harvesting of the solar energy.

The bandgap of CdS QDs can also be calculated using effective mass model.[39,40] It is the simplest model, which predicts the effective bandgap (E_g^*) due to three dimensional confinements. The blue shift of the bandgap with decrease in dot size is described by the following equation:

$$E_g^* = E_g^{bulk} + \frac{\hbar^2 \pi^2}{2 \mu R^2}, \tag{3}$$

where, E_g^{bulk} is the band gap of bulk CdS, $\hbar = h/2\pi$ (h being Planck's constant), R is the dot size and μ is the effective reduced mass,

$$\mu = \frac{1}{m_o}\left(\frac{1}{m_e^*} + \frac{1}{m_h^*}\right), \tag{4}$$

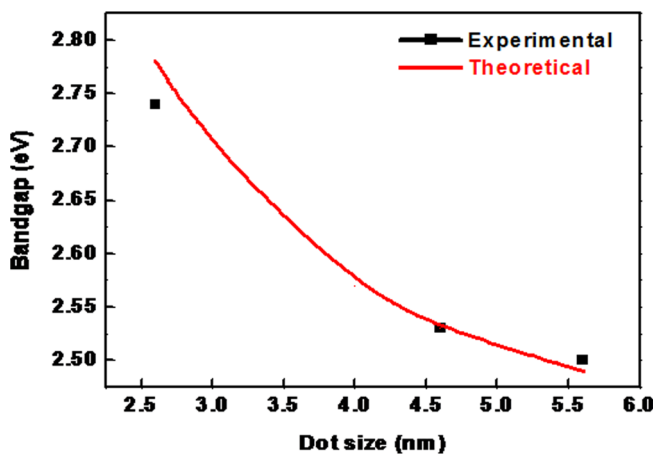

FIG. 10. Experimental and theoretical bandgap of CdS QDs as a function of dot size.

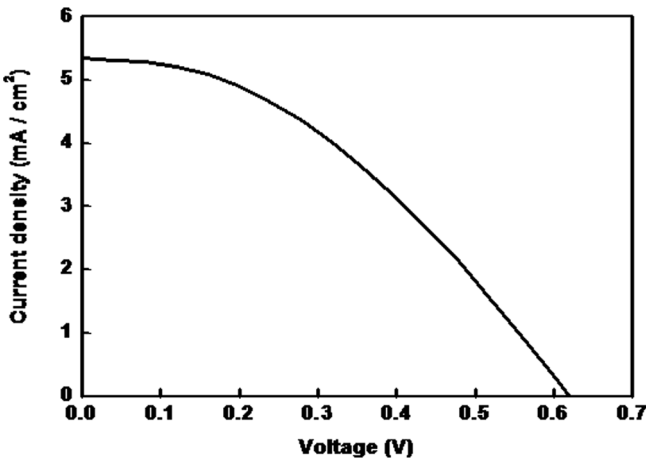

FIG. 11. I-V characteristic of QDSSC.

where, m_o, m_e* (0.2), and m_h* (0.8) are the mass of the electron, effective mass of electron, and effective mass of hole, respectively. The second term in Eq. (3) represents the kinetic energy.[41] The effective bandgap of the CdS QDs is found to be varying from 2.49 to 2.78 eV with decrease in dot size from 5.6 to 2.6 nm, which agrees with the confinement regime. The effective and experimental values of the QD bandgap as a function of dot size are shown in Figure 10. It is clear that the bandgap decreases with increase in the CdS QDs size. This is due to the quantum confinement effect in the dots.[39,40]

C. I-V measurement

QDSSC was fabricated using the synthesized of ZnO NPs and CdS QDs. The cell was illuminated under one sun illumination (AM 1.5, 100 mW/cm^2) and I-V characteristic of the cell (Figure 11) was obtained by using Keithley source meter. The values of short circuit current (I_{sc}), open circuit voltage (V_{oc}), maximum power (P_m), fill factor (FF), and efficiency (η) are 5.43 mA, 0.64 V, 1.3 mW, 0.4 and 1.3%, respectively. When the QDSSC is illuminated, excitons are generated in CdS QDs and charge separation is performed by ZnO/CdS QDs/electrolyte interface. The resultant electrons are conducted to the ITO layer through ZnO layer and the holes are recovered by I^-/I_3^- electrolyte. I_{sc} depends on number of incident photons. Adsorbing PVA capped CdS onto ZnO could result in the hindrance of charge transport. In the present case, the PVA capping molecules were removed by repeated washing[30] with DI water before incorporating them in ZnO electrode in QDSSC, which provides a better charge carrier exchange between QDs and the conducting polymer. The overall conversion efficiency is found to be 1.3%.

IV. CONCLUSION

In conclusion, ZnO based QDSSC with an efficiency of 1.3% at AM 1.5 has been successfully fabricated by sensitizing the ZnO electrode by CdS QDs. The CdS QDs of varying size from 5.6 to 2.6 nm with increase in the bandgap from 2.5 to 2.74 eV, respectively, have been chemically synthesized. The use of QDs of varying bandgap resulted in the absorbance of a broader spectrum of visible light in the range 400–600 nm.

ACKNOWLEDGMENTS

This work is done under DST-JSPS sponsored project No. DST/INT/JSPS/PROJ/10. One of the authors, Neetu Singh, gratefully acknowledges the financial support by University Grant Commission (UGC) in the form of JRF. The authors are also thankful to University Science Instrumentation Centre (USIC) for providing XRD and TEM facilities.

[1]D. R. Baker and P. V. Kamat, Adv. Funct. Mater. 19, 805 (2009).
[2]M. Gratzel, J. Photochem. Photobiol. C **4**, 145 (2003).
[3]C. Longo and M.-A. D. Paoli, J. Braz. Chem. Soc. **14**, 889 (2003).
[4]S. Dai, J. Weng, Y. Sui, S. Chen, S. Xiao, Y. Huang, F. Kong, X. Pan, L. Hu, C. Zhang, and K. Wang, Inorg. Chim. Acta **361**, 786 (2008).
[5]M. Wang, C. Huang, Y. Cao, Q. Yu, Z. Deng, Y. Liu, Z. Huang, J. Huang, Q. Huang, W. Guo, and J. Liang, J. Phys. D: Appl. Phys. **42**, 155104 (2009).
[6]Y. Lee, B. Huang, and H. Chien, Chem. Mater. **20**, 6903 (2008).
[7]K. S. Leschkies, R. Divakar, J. Basu, E. Enache-Pommer, J. E. Boercker, C. B. Carter, U. R. Kortshagen, D. J. Norris, and E. S. Aydil, Nano lett. **7**, 1793 (2007).
[8]J. B. Sambur, T. Novet, and B. A. Parkinson, Science **330**, 63 (2010).
[9]P. Sudhagar, J. H. Jung, S. Park, R. Sathyamoorthy, H. Ahn, and Y. S. Kang, Electrochim. Acta **55**, 113 (2009).
[10]C. Chang and Y. Lee, Appl. Phys. Lett. **91**, 053503 (2007).
[11]Y. Zhang, T. Xie, T. Jiang, X. Wei, S. Pang, X. Wang, and D. Wang, Nanotechnology **20**, 155707 (2009).
[12]Y. Tak, H. Kim, D. Lee, and K. Yong, Chem. Commun. **38**, 4585 (2008).
[13]J. Lee, Y. Sung, T. G. Kim, and H. Choi, Appl. Phys. Lett. **91**, 113104 (2007).
[14]J. Chen, J. Wu, W. Lei, J. L. Song, W. Q. Deng, and X. W. Sun, Appl. Surf. Sci. **256**, 7438 (2010).
[15]N. Daneshvar, S. Aber, M. S. Seyed Dorraji, A. R. Khataee, and M. H. Rasoulifard, Int. J. Chem. Biological Eng. **1**(1), 23 (2008).
[16]D. Chen, X. Jiao, and G. Cheng, Solid State Commun. **113**, 363 (2000).
[17]B. Suo, X. Su, J. Wu, D. Chen, A. Wang, and Z. Guo, Mater. Chem. Phys. **119**, 237 (2010).
[18]P. Suri and R. M. Mehra, Sol. Energy Mater. Sol. Cells **91**, 518 (2007).
[19]S. Rani and R. M. Mehra, J. Renewable Sustainable Energy **1**, 033109 (2009).
[20]J. Chen, J. L. Song, X. W. Sun, W. Q. Deng, C. Y. Jiang, W. Lei, J. H. Huang, and R. S. Liu, Appl. Phys. Lett. **94**, 153115 (2009).
[21]C. Luan, A. Vaneski, A. S. Susha, X. Xu, H. E. Wang, X. Chen, J. Xu, W. Zhang, C. Lee, A. L. Rogach, and J. A. Zapien, Nanoscale Res. Lett. **6**, 340 (2011).
[22]S. Leschkies, R. Divakar, J. Basu, E. Enache-Pommer, J. E. Boercker, C. B. Carter, U. R. Kortshagen, D. J. Norris, and E. S. Aydil, Nano Lett. **7**, 1793 (2007).
[23]P. V. Kamat, J. Phys. Chem. C **112**, 18737 (2008).
[24]H. Zhang, G. Chen, G. Yang, J. Zhang, and X. Lu, J. Mater. Sci: Mater. Electron. **18**, 381 (2007).
[25]Y. Zhu and Y. Zhou, Appl. Phys. A **92**, 275 (2008).
[26]N. Goswami and D. K. Sharma, Physica E **42**, 1675 (2010).
[27]M. Maleki, M. S. Ghamsari, Sh. Mirdamadi, and R. Ghasemzadeh, Semiconductor Physics, Quantum Electronics & Optoelectronics **10**, 30 (2007).
[28]M. J. Pawar and S. S. Chaure, Chalcogenide Lett. **6**, 689 (2009).
[29]P. Nandakumar and C. Vijayan, J. Appl. Phys. **19**, 1509 (2002).
[30]D. V. Talapin, S. K. Poznyak, N. P. Gaponik, A. L. Rogach, and A. Eychmuller, Physica E **14**, 237 (2002).
[31]A. V. Firth, S. W. Haggata, P. K. Khanna, S. J. Williams, J. W. Allen, S. W. Magennis, I. D. W. Samuel, and D. J. Cole-Hamilton, J. Lumin. **109**, 163 (2004).
[32]X. Ma, X. Qian, J. Yin, and Z. Zhu, J. Mater. Chem. **12**, 663 (2002).
[33]L. Han, D. Qin, X. Jiang, Y. Liu, L. Wang, J. Chen, and Y. Cao, Nanotechnology **17**, 4736 (2006).
[34]P. K. Khanna, R. R. Gokhale, V. V. V. S. Subbarao, N. Singh, K. W. Jun, and B. K. Das, Mater. Chem. Phys. **94**, 454 (2005).
[35]J. Kuljanin-Jakovljevic. Z. Stojanovic, and J. M. Nedeljkovic, J. Mater. Chem. Phys. **41**, 5014 (2006).
[36]H. Yao and N. Kitamura, Bull. Chem. Soc. Jpn. **69**, 1227 (1996).
[37]E. A. Meulenkamp, J. Phys. Chem. B **102**, 5566 (1998).
[38]U. Koch, A. Fojtik, H. Weller, and A. Henglein, Chem. Phys. Lett. **122**, 507 (1985).
[39]L. E. Brus, J. Chem. Phys. **80**, 4403 (1984).
[40]S. S. Narayanan and S. K. Pal, J. Phys. Chem. B **110**, 24403 (2006).
[41]P. Gupta and M. Ramakhiani, Open Nanosci. J. **3**, 15 (2009).